

# Efficient High-Fidelity Simulation of Multibody Systems with Composite Dimensionally Reducible Components

Wenbin Yu

*Assistant Professor,*

*Utah State University,*

*Logan, Utah*

## Abstract

This paper introduces a new concept for simulating multibody systems with composite dimensionally reducible components using efficient high-fidelity models of VABS and VAPAS which are constructed using the variational asymptotic method. A systematic theoretical framework is given to connect these efficient high-fidelity models with multibody simulation codes. Several examples including buckling/postbuckling, free/forced vibrations, and simple multibody systems are used to demonstrate connection between DYMORE and VABS/VAPAS. It is shown that various types of analyses can be handled using the same approach and the same structure can be analyzed using different models based on required accuracy and efficiency. It is shown that effects of boundary conditions should be carefully examined when comparing different models. It is concluded that realistic engineering systems involving composite components can be authentically yet efficiently simulated using flexible multibody codes along with the efficient high-fidelity models provided in VABS and VAPAS.

---

Presented at the 46th Structures, Structural Dynamics and Materials Conference, Austin, Texas, April 18–21, 2005.

## Introduction

During the last decade, there have been significant advance made in the general-purpose modeling of multibody dynamic systems in general, rotorcraft in particular. The state of the art is embodied in powerful comprehensive codes such as CAMRAD II, DYMORE, and RCAS. The predictive capabilities of such codes heavily rely on the models used for various components. Most of modern multibody systems have components made of composites, such as composite rotor blades, composite flexbeams of rotorcraft. Accurate yet efficient models for composite structures are indispensable for engineers to use comprehensive multibody codes to efficiently yet confidently simulate systems involving composite components.

Most of composite components in engineering systems are so-called dimensionally reducible structures with some dimensions much larger than the others. For example, composite beams have one dimension (the axial direction) much larger than the cross-sectional dimensions, and composite plates/shells have two dimensions (the in-plane directions) much larger than the thickness. Analysts are striving to develop reduced-order models to simplify the analysis of such structures by taking advantage of the smallness of smaller dimensions. Although there exist many theories addressing the complexity of composite structures introduced by anisotropy and heterogeneity of composite materials (Refs. 1–3), engineers are reluctant to accept them with confidence because most theories are either oversimplified without acceptable accuracy, such as the classical lamination theories (CLT) or the first-order shear-deformation theories (FOSDT), or too complicated to be used efficiently to meet the time constraints of design and analysis, such as higher-order layer-wise theories. Furthermore, many theories are developed for specific materials, layups, geometries, or analyses, and cannot be easily generalized to allow the designer to have full control of the optimization of all these aspects. An integrated approach with sufficient efficiency and accuracy, accounting for all the deformations, general enough to handle arbitrary materials, layups, geometries and all types of structural behavior (such as deformation, stress analysis, buckling, and vibration), is needed to exploit the full potential of composite materials.

Although it is understood that all reduced-order models of composite structures are inherently approximate, the hypothesis used to derive such models should be carefully examined, particularly *ad hoc* assumptions without reasonable justifications should be avoided or minimized. For example, for geomet-

rically nonlinear analysis, it is reasonable to assume that the strains are small. However, it is not at all reasonable to assume *a priori* some *ad hoc* displacement field although, unfortunately, that is the way most reduced models of composite structures have been constructed.

Recently, variational asymptotic structural analysis (VASA) has emerged to be a new paradigm of modelling composite structures based on the variational asymptotic method (VAM) introduced by Berdichevsky (Ref. 4). A series of high-fidelity models for composite beams (Refs. 5, 6), composite plates (Refs. 7, 8), and composite shells (Ref. 9) have been developed without invoking any *ad hoc* kinematic assumptions. These models are as simple as traditional engineering models (such as the Euler-Bernoulli model or the Timoshenko model for beams, and the Kirchhoff-Love model or the Reissner-Mindlin model for plates and shells) with much better accuracy, *i.e.*, an excellent compromise between accuracy and efficiency has been achieved in these new models of composite structures. These theories have been implemented in two finite-element based computer programs: VABS (variational asymptotic beam sectional analysis) and VAPAS (variational asymptotic plate and shell analysis). VABS and VAPAS can provide constitutive models for beam elements and plate/shells elements which are available in flexible multibody codes, respectively. Both codes can accurately recover the three-dimensional (3D) distribution of displacements, stresses, and strains within the original structures. To fully take advantage of VABS and VAPAS, the beam/plate/shell elements should be able to accept fully populated stiffness matrices including all possible couplings between all the fundamental deformations represented by the reduced model.

In this paper, we will first provide the theoretical foundation to connect VABS/VAPAS with flexible multibody codes. Then, several examples including buckling, free vibration, forced vibration, and simple multibody systems are analyzed using DYMORE with structural models provided by VABS/VAPAS to demonstrate the efficiency, accuracy, and versatility of this approach.

### **Theoretical Foundation**

If we consider composite structures as elastic bodies, their behavior is completely determined by the elastic energy. Therefore, to construct reduced models for dimensionally reducible structures, we need to answer: “how can we reproduce the elastic energy of the 3D formulation using the reduced models?” The

most common approach to this problem is to invoke *ad hoc* kinematic assumptions. For example, for most of composite beam models, the 3D displacements are assumed to be expressed in terms of known functions of the cross section and unknown 1D variables defined over the beam reference line. Because of its simplicity and inherent variational nature, this approach is extensively used in the engineering community despite of the fact that the adopted assumptions either clearly violate the original 3D formulation or cannot be reasonably justified.

Fundamentally, theories of composite structures can be derived from a variational statement of the original 3D problem based on the Hamilton's principle for elastodynamics of anisotropic bodies such as:

$$\delta \int_t \int_V \mathcal{L} dV dt + \int_t \overline{\delta W} dt = 0 \quad (1)$$

where  $\delta$  is the variation symbol,  $\mathcal{L}$  is the Lagrangian containing the kinetic energy and the internal energy of the composite structure, and  $\overline{\delta W}$  is the virtual work done by applied loads through virtual displacements. The internal energy of the structure can be obtained using the 3D constitutive relations relating stresses and strains. For example, for linear elastic material, we have

$$\sigma_{ij} = c_{ijkl} \epsilon_{kl} \quad (2)$$

where  $\sigma_{ij}$  denote the stress components and  $\epsilon_{ij}$  denote the strain components and  $c_{ijkl}$  are the material constants obtained outside the theory by experiments or micromechanics analysis. Here and through the paper Latin indices assume 1, 2, and 3. Repeated indices are summed over their range except where explicitly indicated.

This stationary value problem in Eq. (1) can be solved analytically for highly idealized situations such as the well-known cylindrical bending problem (Ref. 10). For general cases, the 3D finite element method is often used for numerical solutions if computational cost and efficiency are not critical issues. Otherwise, we need to reduce the dimensionality of the problem so that a meaningful solution with reasonable accuracy can be obtained with less efforts and resources. The validity of the latter alternative has been demonstrated by the success of theories of beams/plates/shells in design and analysis of structures, and it is consistent with the modeling philosophy because even the original 3D formulation in Eq. (1) can be considered as a reduced model from the quantum mechanics model of a discrete system containing many atoms, which itself a model of matter.

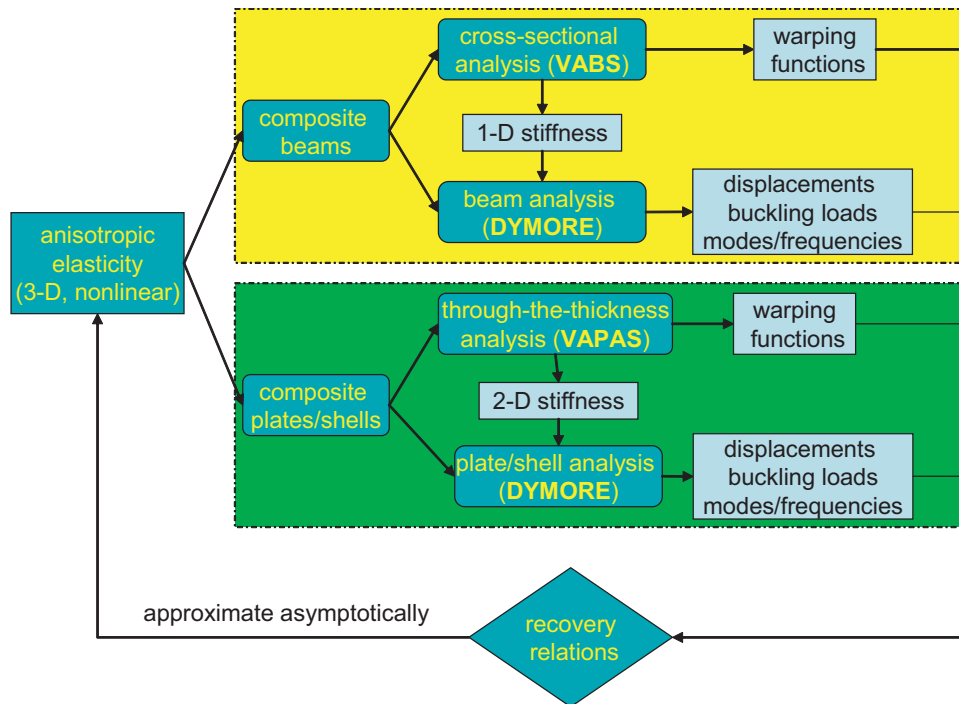


**Fig. 1** Variational asymptotic analysis of composite dimensionally reducible components.

Instead of relying on *ad hoc* kinematical assumptions to reduce the dimensionality of Eq. (1), VASA takes advantage of the small parameters inherent in the structure to systematically carry out the dimensional reduction. The mathematical foundation of VASA is VAM, a powerful technique to simplify the procedure of solving problems governed by variational statements involving one or more small parameters. In contrast to conventional asymptotic methods, VAM carries out asymptotic analysis of the variational statement. Therefore, VAM is synthesis of both merits of variational methods (*viz.*, systematic, simple, and easy to be implemented numerically), and asymptotic methods (*viz.*, without *ad hoc* kinematic assumptions). The accuracy of models constructed using VAM is guaranteed by the asymptotic analysis (*i.e.*, the results obtained by VAM converges asymptotically to the exact solutions) and the approximate formulation is always variational such that it is easier than conventional asymptotic analysis to prove the asymptotic correctness of the approximate formulation and implement it numerically. Interested readers should refer to Refs. 4, 11 for the details of VAM.

The basic steps of VASA is illustrated in Fig. 1. The original 3D bodies of composite dimensionally reducible components can be classified as beams, plates, or shells according to their geometric charac-

teristics. The unique feature of VASA is to use VAM to mathematically split the original 3D nonlinear problem into a set of local analyses over small dimensions and a set of global analyses over the large dimensions. This decoupling allows the global analyses to be formulated exactly and intrinsically as a general 1D continuum for beams and a 2D continuum for plates/shells and confines all the approximations to the local analysis over small dimensions, the accuracy of which is guaranteed to be the best by VAM.

For composite beams, we can use the VAM to split the nonlinear 3D anisotropic elasticity problem into a two-dimensional (2D), linear, cross-sectional analysis and a one-dimensional (1D) nonlinear beam analysis for the reference line with the help of small geometrical parameters  $h/l$  and  $h/R$  (where  $h$  is the characteristic size of the section,  $l$  the characteristic wavelength of axial deformation and  $R$  the characteristic radius of initial curvatures and twist of the beam). The cross-sectional analysis is implemented in the computer program VABS using 2D finite elements. VABS can provide various 1D constitutive models corresponding to different approximations of the original 3D problem. From the first approximation, one can obtain the Euler-Bernoulli model (also called classical beam model) represented by a  $4 \times 4$  stiffness model as follows:

$$\begin{pmatrix} F_1 \\ M_1 \\ M_2 \\ M_3 \end{pmatrix} = \begin{bmatrix} S_{11} & S_{12} & S_{13} & S_{14} \\ S_{12} & S_{22} & S_{23} & S_{24} \\ S_{13} & S_{23} & S_{33} & S_{34} \\ S_{14} & S_{24} & S_{34} & S_{44} \end{bmatrix} \begin{pmatrix} \gamma_{11} \\ \kappa_1 \\ \kappa_2 \\ \kappa_3 \end{pmatrix} \quad (3)$$

where  $\gamma_{11}$  is the extension,  $\kappa_1$  is twist,  $\kappa_2$  and  $\kappa_3$  are bending curvatures along  $x_2$  and  $x_3$ , respectively,  $F_1$  and  $M_i$  are the corresponding stress and moment resultants, and  $S_{11}, \dots, S_{44}$  are sectional stiffness constants. Eq. (3) can be viewed as 1D version of Eq. (2) which can be used to obtain a 1D variational statement as the first approximation of the original 3D variational statement in Eq. (1) for composite beams.

The classical model works pretty well for slender beams which do not have thin-walled open sections and undergo motions with large wavelength. However, refined theories are required for better prediction when the beam is fat, or has thin-walled open sections, or vibrates in short-wavelength modes. To obtain a refined beam model, one needs to carry out the variational asymptotic analysis of the variational statement

one more step to obtain an internal energy asymptotically correct up to the order of  $(h/\ell)^2$  and  $(h/R)^2$ . The model obtained directly using VAM involves derivatives of the 1D strains and cannot be applied conveniently in real applications. We can transform the asymptotically correct model into beam models commonly used in engineering practice. VABS provides a generalized Timoshenko beam model (Ref. 12) to treat transverse shear deformation which becomes significant for fat beams or beams vibrating in higher frequencies:

$$\begin{Bmatrix} F_1 \\ F_2 \\ F_3 \\ M_1 \\ M_2 \\ M_3 \end{Bmatrix} = \begin{bmatrix} S_{11} & S_{12} & S_{13} & S_{14} & S_{15} & S_{16} \\ S_{12} & S_{22} & S_{23} & S_{24} & S_{25} & S_{26} \\ S_{13} & S_{23} & S_{33} & S_{34} & S_{35} & S_{36} \\ S_{14} & S_{24} & S_{34} & S_{44} & S_{45} & S_{46} \\ S_{15} & S_{25} & S_{35} & S_{45} & S_{55} & S_{56} \\ S_{16} & S_{26} & S_{36} & S_{46} & S_{56} & S_{66} \end{bmatrix} \begin{Bmatrix} \gamma_{11} \\ 2\gamma_{12} \\ 2\gamma_{13} \\ \kappa_1 \\ \kappa_2 \\ \kappa_3 \end{Bmatrix} \quad (4)$$

where  $2\gamma_{12}$  and  $2\gamma_{13}$  are the transverse shear strains and  $F_2$  and  $F_3$  the corresponding stress resultants.

To analyze thin-walled beams with open sections, we need to consider the effect of nonuniform warping and transform the refined asymptotically correct model into a generalized Vlasov beam model (Ref. 13):

$$\begin{Bmatrix} F_1 \\ M_1 \\ M_2 \\ M_3 \\ M_\omega \end{Bmatrix} = \begin{bmatrix} S_{11} & S_{12} & S_{13} & S_{14} & S_{15} \\ S_{12} & S_{22} & S_{23} & S_{24} & S_{25} \\ S_{13} & S_{23} & S_{33} & S_{34} & S_{35} \\ S_{14} & S_{24} & S_{34} & S_{44} & S_{45} \\ S_{15} & S_{25} & S_{35} & S_{45} & S_{55} \end{bmatrix} \begin{Bmatrix} \gamma_{11} \\ \kappa_1 \\ \kappa_2 \\ \kappa_3 \\ \kappa'_1 \end{Bmatrix} \quad (5)$$

where  $M_\omega$  is so-called bimoment conjugate to twist rate  $\kappa'_1$ .

All these models are available in the current version of VABS. Additional details can be found in Refs. 5, 6, 12, 13. These constitutive models can be used as inputs for any generalized beam elements with the same definition of 1D strains as VABS to carry out all kinds of global beam analyses including geometrically nonlinear analyses. Finally the global behavior obtained in the beam analyses can be used along with the sectional warping functions to recover the 3D distribution of displacements/stresses/strains within the original structure. Thus, we can find an approximate solution for Eq. (1) for beam type struc-

tures using three steps: a) obtain sectional constitutive models and sectional warping functions using VABS; b) carry out global beam analyses using the obtained sectional constitutive models; c) recover the 3D results based on the global responses and sectional warping functions using VABS.

As shown in Fig. 1, we can decouple the original 3D problem of composite plates/shells into a 1D, linear, through-the-thickness analysis and a 2D, nonlinear, plate/shell analysis using the VAM with the aid of small geometrical parameters  $h/l$  and  $h/R$  (where  $h$  is the thickness,  $l$  the characteristic wavelength of deformation in the reference surface and  $R$  the characteristic radius of initial curvatures of shells). The through-the-thickness analysis is implemented in VAPAS using the finite element method. For the first approximation, VAPAS will calculate a generalized 2D constitutive model in the form of Kirchhoff-Love theory of the plate/shell:

$$\begin{Bmatrix} N \\ M \end{Bmatrix} = \begin{bmatrix} A & B \\ B^T & D \end{bmatrix} \begin{Bmatrix} \epsilon \\ \kappa \end{Bmatrix} \quad (6)$$

where  $N^T = [N_{11} \ N_{12} \ N_{22}]$  is the vector of in-plane forces per unit length and  $\epsilon^T = [\epsilon_{11} \ 2\epsilon_{12} \ \epsilon_{22}]$  the corresponding in-plane strains;  $M^T = [M_{11} \ M_{12} \ M_{22}]$  is the vector of bending moments per unit length and  $\kappa^T = [\kappa_{11} \ 2\kappa_{12} \ \kappa_{22}]$  the corresponding curvatures. The  $A$ ,  $B$ , and  $D$  matrices are the same as those of CLT. However, no *ad hoc* kinematic assumptions associated with CLT, such as the transverse normal line remains as the normal line after deformation and transverse normal is infinitely rigid in the thickness direction, have been used to derive this model. For shells,  $A$ ,  $B$ , and  $D$  will also be corrected by the initial curvatures (Ref. 9).

The Reissner-Mindlin model can be obtained from the next approximation of VAPAS by including all the terms up to the order of  $(h/l)^2$  in the original 3D formulation, Eq. (1). Again, VAPAS will meet the same difficulty as VABS because the refined asymptotically correct model includes derivatives of strain measures which is not a convenient model for engineers. We can use optimization techniques to transform the asymptotical model into an engineering model such as the Reissner-Mindlin model

$$\begin{Bmatrix} N \\ M \\ Q \end{Bmatrix} = \begin{bmatrix} A & B & C \\ B^T & D & E \\ C^T & E^T & G \end{bmatrix} \begin{Bmatrix} \epsilon \\ \kappa \\ \gamma \end{Bmatrix} \quad (7)$$

where  $Q^T = [Q_{13} \ Q_{23}]$  is the vector of transverse shear forces per unit length and  $\gamma^T = [2\gamma_{13} \ 2\gamma_{23}]$  the

corresponding transverse shear strains.  $G$  is the transverse shear stiffness matrix. The VAPAS Reissner-Mindlin model is of the same form of FOSDT. However, no *ad hoc* kinematic assumptions associated with FOSDT are used and no shear correction factors are necessary for calculation of  $G$ .

After obtaining these 2D constitutive models, one can use them as inputs for any generalized plate/shell elements, providing these elements have the same definition of 2D strains as VAPAS, to carry out all kinds of global plate/shell analyses. The through-the-thickness distribution can be recovered based on the global responses from global plate/shell analyses and the warping functions calculated by VAPAS. Therefore, we can seek an approximate solution for Eq. (1) for composite plate/shells using three steps: a) obtain plate/shell constitutive models and warping functions using VAPAS; b) carry out global plate/shell analyses using the obtained constitutive models; c) recover the 3D results based on the global responses and warping functions using VAPAS.

### Numerical Examples

The Timoshenko model of VABS, and the Reissner-Mindlin model of VAPAS are seamlessly linked with DYMORE beam elements and shells elements, respectively. In this section, we are going to carry out various simulations using DYMORE to demonstrate the accuracy and usage of high-fidelity models obtained using VABS and VAPAS. Since the linear static deformation and recovered 3D results have been reported in publications related with VABS and VAPAS, in this study, we will instead focus on the global responses, including both dynamic behavior and geometrically nonlinear behavior, of the composite structures using DYMORE with VABS Timoshenko model (we label it as the “Beam” approach) and using DYMORE with VAPAS Reissner-Mindlin model (we label it as the “Plate” approach). The results are compared with those available in the literature and the 3D finite element method using ANSYS.

#### Free vibration of a rectangular composite beam

The first example is a cantilevered graphite-epoxy beam of rectangular sections with 30° layup orientation. The material properties of graphite-epoxy and the dimensions of the structure are listed in Table 1. The free vibration of this beam has been studied extensively in the literature by Abarcar and Cunniff

**Table 1.** Material properties and dimensions of the rectangular graphite-epoxy beam

$E_{11}$	$18.73 \times 10^6$ psi
$E_{22}$	$1.364 \times 10^6$ psi (= $E_{33}$ )
$G_{12}$	$0.7479 \times 10^6$ psi
$G_{13}$	$0.6242 \times 10^6$ psi
$G_{23}$	$0.3686 \times 10^6$ psi
$\nu_{12}$	0.3 (= $\nu_{13} = \nu_{23}$ )
$\rho$	$1.450 \times 10^{-4}$ lb.sec <sup>2</sup> /in. <sup>4</sup>
Width	0.5 in.
Thickness	0.125 in.
Length	7.5 in.

(Ref. 14), Hodges *et al.* (Ref. 15), Jung *et al.* (Ref. 16), and Mitra *et al.* (Ref. 17), along with others.

The cross section is meshed with 5 8-noded quadrilateral elements along the thickness and 20 8-noded quadrilateral elements along the width. The sectional mass properties obtained by VABS are

$$\begin{aligned}
 \mu &= 0.9063 \times 10^{-5} \text{ lb.sec}^2/\text{in.}^2 \\
 i_2 &= 0.1180 \times 10^{-7} \text{ lb.sec}^2 \\
 i_3 &= 0.1888 \times 10^{-6} \text{ lb.sec}^2
 \end{aligned} \tag{8}$$

where  $\mu$  is the mass per unit length and  $i_2$  is the mass moments of inertia about the direction along the width and  $i_3$  is the mass moments of inertia about the direction along the thickness. The sectional stiffness constants obtained using VABS are listed in Table 2. Clearly this composite beam exhibits extension-shear coupling and torsion-bending coupling. Although VABS allows users to use their own unit system, it is recommended to be consistent in the unit system to avoid any possible mistakes in the conversion of units.

Now we are ready to use DYMORE to carry out the free vibration analysis of this composite beam. For this global beam analysis, we mesh the reference line with 20 quadratic beam elements, the natural

**Table 2.** The stiffness of Timoshenko model of the rectangular graphite-epoxy beam

Stiffness	VABS Results
$S_{11}$	$0.3566 \times 10^6$ (lb)
$S_{12}$	$0.1274 \times 10^6$ (lb)
$S_{22}$	$0.1005 \times 10^6$ (lb)
$S_{33}$	$0.8634 \times 10^4$ (lb)
$S_{44}$	$0.5069 \times 10^3$ (lb-in <sup>2</sup> )
$S_{45}$	$-0.3215 \times 10^3$ (lb-in <sup>2</sup> )
$S_{55}$	$0.4578 \times 10^3$ (lb-in <sup>2</sup> )
$S_{66}$	$0.4062 \times 10^4$ (lb-in <sup>2</sup> )

**Table 3.** Natural frequencies (Hz) of the rectangular graphite-epoxy beam

Mode	Ref. 14	Ref. 15	Ref. 16	Ref. 17	Beam	Plate	ANSYS
1 (FT)	52.7	49.0	52.7	52.8	52.6	54.6	54.4
2 (LB)	N/A	195.6	210.7	210.0	209.8	214.5	214.3
3 (FT)	331.8	307.9	329.2	329.5	326.3	340.4	339.7
4 (FT)	924.7	869.1	918.6	916.1	899.8	949.1	947.1
5 (LB)	N/A	1215.2	1320.4	1263.9	1284.9	1318.9	1317.4
6 (FT)	1766.9	N/A	1762.9	1756.0	1661.3	1687.1	1685.5
7 (TF)	1827.4	1660.9	1836.6	1858.0	1744.8	1860.5	1857.5
8 (FT)	2984.0	N/A	2944.6	2909.6	2782.9	3043.7	3038.5

**Table 4.** The stiffness of Reissner-Mindlin model of the rectangular graphite-epoxy beam

Stiffness	VAPAS Results
$A_{11}$	$0.1426 \times 10^7$ (lb/in.)
$A_{12}$	$0.6952 \times 10^6$ (lb/in.)
$A_{13}$	$0.4361 \times 10^6$ (lb/in.)
$A_{22}$	$0.4781 \times 10^6$ (lb/in.)
$A_{23}$	$0.2510 \times 10^6$ (lb/in.)
$A_{33}$	$0.3326 \times 10^6$ (lb/in.)
$G_{11}$	$0.5875 \times 10^5$ (lb/in.)
$G_{12}$	$0.1132 \times 10^5$ (lb/in.)
$G_{22}$	$0.4596 \times 10^5$ (lb/in.)

frequencies calculated by DYMORE are compared with other published results in Table 3, where Ref. 14 represents the results of the experimental study of Abarcar and Cunniff and Beam represents the results using DYMORE with VABS Timoshenko model. In Table 3, the first eight modes including the first five flap-torsion (FT) modes, the first two lag bending (LB) modes, and the first torsion-flap modes are presented. It can be observed for the first three natural frequencies all the results except those of Ref. 15 have very good agreement with a difference less than 1.5% and the results of Ref. 15 are consistently lower than others. For higher frequencies, the results obtained using DYMORE with VABS are located between the scattering of the reported results in the literature.

We can also use DYMORE with VAPAS Reissner-Mindlin plate model to analyze the same structure. The through-the-thickness finite element model has only one 5-noded line element. From VAPAS, we obtain the mass per unit area  $0.1813 \times 10^{-4}$  lb.sec<sup>2</sup>/in<sup>3</sup>, mass center at the center of the thickness, and radius of gyration  $\rho_g = 0.3608 \times 10^{-1}$  in. The plate stiffness constants obtained using VAPAS are listed in Table 4 and  $D = h^2/12A$  with  $h$  as the thickness in the unit of inch. We mesh the reference plane using 20 quadratic quadrilateral elements along the length and 5 quadratic quadrilateral elements along

**Table 5.** Sensitivity of natural frequencies (Hz) using different boundary conditions

Mode	B1	B2	B3	B4
1 (FT)	54.4	53.9	53.5	43.1
2 (LB)	214.3	211.0	203.7	148.8
3 (FT)	339.7	336.6	333.9	284.8
4 (FT)	947.1	938.9	932.1	819.5
5 (LB)	1317.4	1298.2	1258.0	1069.0
6 (FT)	1685.5	1673.6	1666.7	1441.3
7 (TF)	1857.5	1844.4	1835.0	1718.5
8 (FT)	3038.5	3011.7	2992.5	2725.0

the width. The results obtained using DYMORE with VAPAS model are also listed in Table 3 and denoted as Plate. It can be observed that the natural frequencies calculated using VAPAS plate model are higher than the corresponding values obtained using VABS beam model. Since both VABS and VAPAS are reduced from 3D formulation, it will be interesting to compare these results with a 3D finite element code, such as ANSYS. We mesh this composite beam using 2000 ANSYS *solid 186* elements with aspect ratio length:width:thickness=15:1:1, which means we divide the length into 20 segments, and maintain the discretization of the section the same as the finite element model for VABS. The ANSYS results listed in Table 3 are obtained by constraining all the degrees of freedom (DOFs) of the root surface. It can be observed that the results obtained using DYMORE with VAPAS agrees with the ANSYS results better than those obtained using DYMORE with VABS, which is logical because VAPAS eliminates one dimension of the 3D structure to obtain a plate model yet VABS eliminates two dimensions of the 3D structures to obtain a beam model.

As far as the comparison between Beam results and ANSYS results concerned, it is difficult to draw any decisive conclusion at this point because it is found out that the boundary conditions have significant effects on the natural frequencies. As shown in Table 5, the natural frequencies of the same beam differ

**Table 6.** Natural frequencies (Hz) of the rectangular graphite-epoxy under free-free condition

Mode	Beam	ANSYS	Difference (%)
1	332.5	333.8	0.4
2	905.2	919.0	1.5
3	1317.9	1321.4	0.3
4	1737.1	1792.6	3.1
5	2807.3	2956.9	5.1
6	3349.4	3357.1	0.2
7	3522.5	3560.1	1.1

more than 20% for some modes under different boundary conditions, where for case B1, all the DOFs of the root surface are constrained; for case B2, only the DOFs of the four edges of the root surface are constrained; for case B3, only the DOFs of the two longer edges of the root surface are constrained; for case B4, only the DOFs of the four corner points and the center point of the root surface are constrained. Although how to pose boundary conditions equivalent to the 3D formulation or experimental conditions in reduced models is still an open question, to justify that indeed boundary conditions contribute to the big differences of higher frequencies in Table 3, we can investigate the free vibration of this composite beam under free-free boundary conditions. To eliminate singularities in DYMORE model, one can connect the mid-span to a flexible joint with very small spring constants (we used  $1 \times 10^{-6}$  for this case). The results obtained using ANSYS and DYMORE with VABS model are compared in Table 6 (the rigid body modes are neglected). Clearly the discrepancy between ANSYS and the Beam approach is greatly decreased within 5.1% for the beam vibrating up to a frequency higher than 3500 Hz.

Although similar results are obtained, the efficiencies using different approaches are dramatically different. According to the author's desktop (Pentium 4 with 3 GHz CPU and 1 G RAM), the Beam approach takes 1.2 seconds, the Plate approach takes 2.03 seconds, and ANSYS takes 92 seconds. Clearly, the Beam approach is the most efficient, and even the Plate approach are far more efficient than the 3D calculation

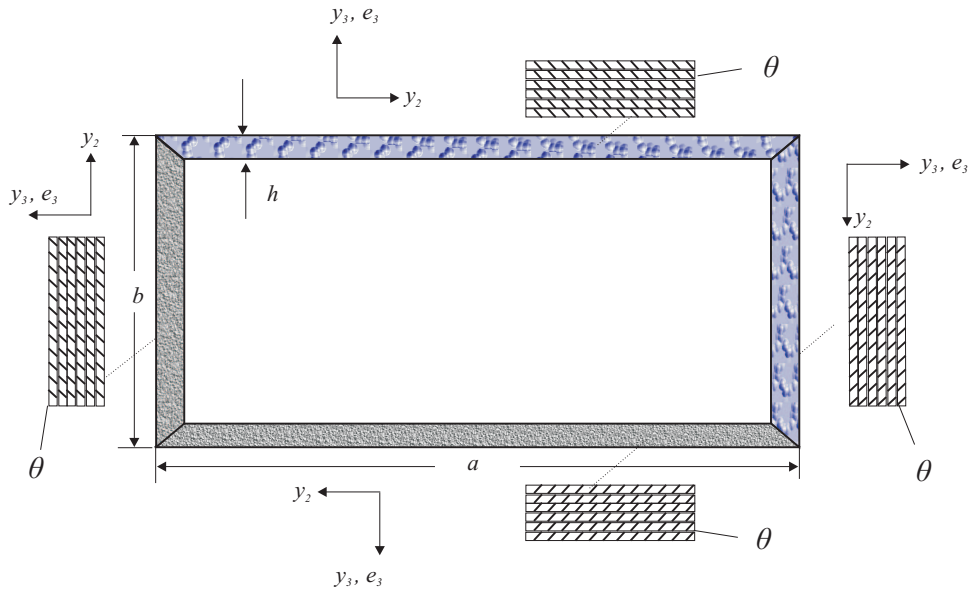


**Fig. 2** Sketch of a box beam with layups

of ANSYS.

**Rotating composite box beam**

The second example is a composite box beam. It has an antisymmetric layer up of  $[15^\circ]_6$  for each wall of the box section. For composite box beams (see Fig. 2), the layup angle is positive for VABS if the fiber rotates from the beam axis around the outward normal of each wall counterclockwise. The stacking sequences can be specified by the users although stacking sequence are usually expressed from the innermost layer to the outermost layer for each wall. The properties of the composite material and dimensions of structure are listed in Table 7.

The cross section is meshed with 336 8-noded quadrilateral elements (16 divisions along the width, 12 divisions along the depth, and 6 divisions through the wall thickness). Sectional mass properties calculated by VABS are

$$\begin{aligned}
 \mu &= 0.1161 \times 10^{-4} \text{ lb.sec}^2/\text{in}^2 \\
 i_2 &= 0.5712 \times 10^{-6} \text{ lb.sec}^2 \\
 i_3 &= 0.1411 \times 10^{-5} \text{ lb.sec}^2
 \end{aligned}
 \tag{9}$$

**Table 7.** Material properties and dimensions of the composite box beam

$E_{11}$	$20.59 \times 10^6$ psi
$E_{22}$	$1.42 \times 10^6$ psi ( $= E_{33}$ )
$G_{12}$	$0.89 \times 10^6$ psi ( $= G_{13} = G_{23}$ )
$\nu_{12}$	0.42 ( $= \nu_{13} = \nu_{23}$ )
$\rho$	$1.353 \times 10^{-4}$ lb.sec <sup>2</sup> /in. <sup>4</sup>
Outer width	0.953 in.
Outer depth	0.537 in.
Wall thickness	0.03 in.
Length	33.25 in.

The sectional stiffness constants of VABS Timoshenko model are listed in Table 8. Intuition tells us that this box beam has extension-twist coupling such that applying a positive axial force would result in a positive twist, which means a positive value for the extension-twist coupling in the flexibility matrix and a negative value in the stiffness matrix. It is noticed that the results reported previously in Refs. 6, 20 were actually calculated using  $[-15^\circ]_6$  based on the current sign convention for the layup angles. The slight difference between the present results and those previously reported in Refs. 6, 20 is due to different meshes and using material properties slightly different from what are listed in Table 7.

The natural frequencies of this box beam rotating around its root surface at a constant angular speed  $\Omega = 1002$  rpm can be calculated using DYMORE by defining a rigid rotation. To carry out the global beam analysis, we mesh the beam axis using 20 quadrilateral beams. The first five modes including the first two flap modes, and the first two lag modes and the first torsion modes are listed in Table 9 and compared with other published results, where the results of Ref. 18 are from experiments. The present results obtained using DYMORE with VABS model have a good correlation with the experimental results and those of other references.

**Table 8.** The stiffness of Timoshenko model of the composite box beam

Stiffness	VABS
$S_{11}$ (lb)	$0.1432 \times 10^7$
$S_{14}$ (lb-in.)	$-0.1060 \times 10^6$
$S_{22}$ (lb)	$0.5104 \times 10^5$
$S_{25}$ (lb-in.)	$0.2947 \times 10^5$
$S_{33}$ (lb)	$0.2129 \times 10^5$
$S_{36}$ (lb-in.)	$0.2988 \times 10^5$
$S_{44}$ (lb-in. <sup>2</sup> )	$0.1696 \times 10^5$
$S_{55}$ (lb-in. <sup>2</sup> )	$0.5510 \times 10^5$
$S_{66}$ (lb-in. <sup>2</sup> )	$0.1365 \times 10^6$

**Table 9.** Natural frequencies (Hz) of a rotating composite box beam ( $[15^\circ]_6$  at  $\Omega = 1002$  rpm)

Mode	Ref. 18	Ref. 19	Ref. 16	Beam	Plate
Flap 1	33.6	36.5	33.9	34.1	33.2
Lag 1	46.6	53.7	45.4	45.9	45.1
Flap 2	184.0	202.2	182.1	181.6	180.6
Lag 2	N/A	328.2	277.5	277.9	278.8
Torsion 1	N/A	493.7	495.5	503.2	491.7

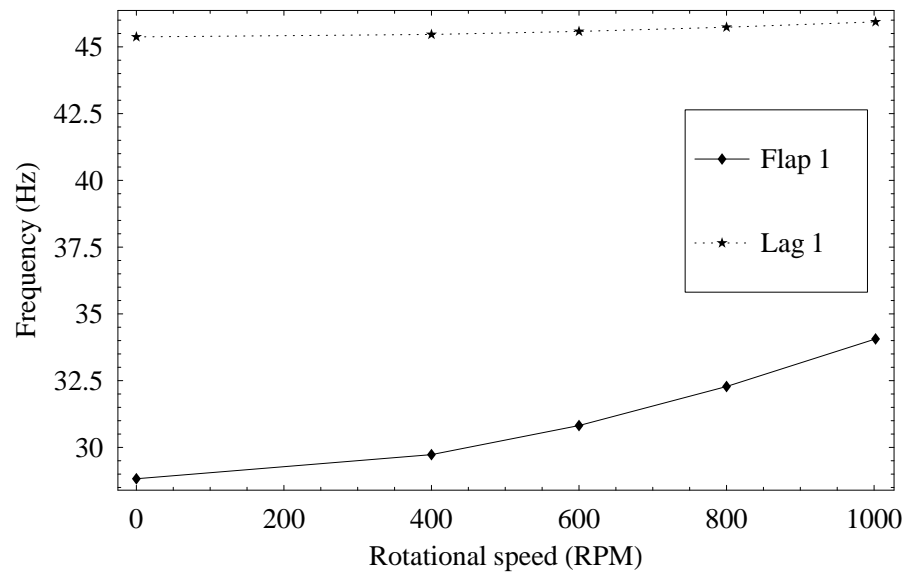


**Fig. 3** Change of natural frequencies with respect to the rotational speed

This box beam can also be analyzed using DYMORE with VAPAS model as four composite plates with same layups connected with each other to form a box. The through-the-thickness analysis using VAPAS is relatively easier than the sectional analysis using VABS, while the global analysis using plate elements is much more difficult than the analysis using beam elements in terms of both building the finite element and computation. The through-the-thickness finite element model has only one 5-noded line element. VAPAS can calculate the mass properties of thickness including mass per unit area, mass center and radius of gyration and Reissner-Mindlin stiffness model. Then we can build a model for DYMORE using plate elements. The DYMORE model is meshed with 320 quadrilateral plate elements. The results of natural frequencies of the rotating box beam calculated using the Plate approach are also listed in Table 9 as a comparison to those obtained using the Beam approach. Although it is desirable to analyze this box beam using 3D elements of ANSYS as what we did for the rectangular composite beam, the size of the problem easily exceeds the nodal limit (128k) of ANSYS academic license because of the large aspect ratios of width/depth to thickness and length to width/depth, and this pursuit cannot be achieved with current resources.

To investigate how natural frequencies of this rotating composite beam are affected by the rotational speed, we plot the natural frequencies calculated using the Beam approach for the first flap mode and first

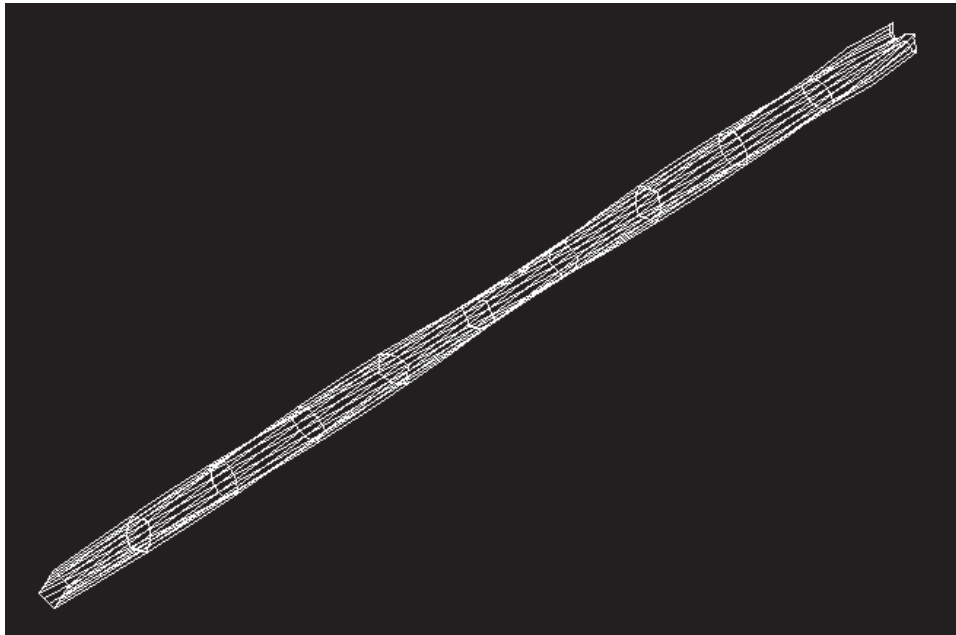


**Fig. 4** The positive extension-twist coupling of the box beam using plate model

lag mode according to different rotational speed in Fig. 3. It is clear that the natural frequency of the first flap mode is affected by the rotational speed significantly, while the rotational speed only affect the first lag mode slightly. The natural frequency of the first flap mode is 28.5 Hz with zero rotation speed. This frequency is increased about 18% when the rotational speed is 1002 rpm.

To verify that the extension-twist coupling exhibited by the Timoshenko stiffness model in Table 8 has the right sign, we analyze the box beam using the Plate approach. Prescribed axial displacements are applied at the corners of the tip surface along the positive axial direction. It is observed from Fig. 4 that indeed this box beam is twisted nose up, implying there is a positive extension-twist coupling coefficient in the flexibility matrix, which further means a negative value for  $S_{14}$  in the stiffness matrix as shown in Table 8.

We can also use the Plate approach to study the buckling behavior of the composite box beam. To avoid collapse of the structure under the critical buckling load, we steadily increase the axial displacement of the tip surface with a strain rate less than  $10^{-3}$ /sec so that the dynamic effects are negligible. Fig. 5 plots change of the vertical displacement ( $u_3$ ) in the middle of the upper wall with respect to the prescribed axial displacement at the tip. It can be observed that this box beam will buckle before it compressed by

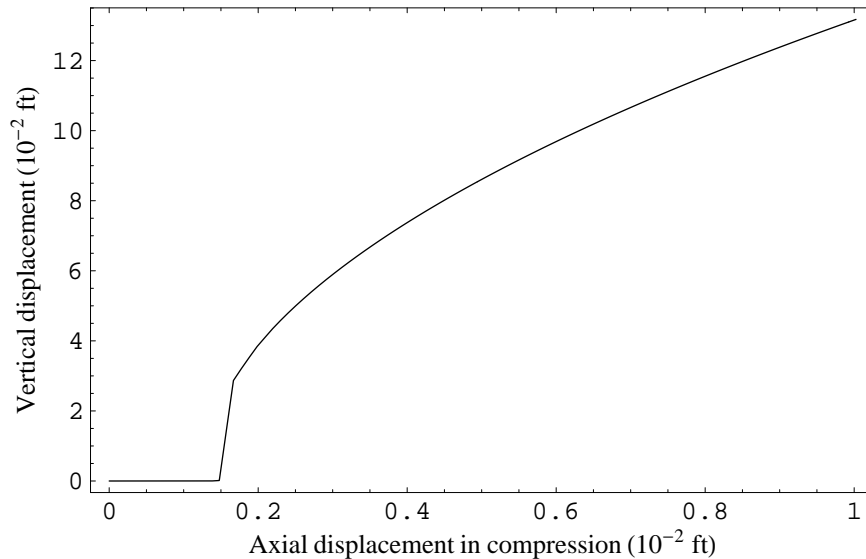


**Fig. 5** Buckling simulation under controlled axial displacement

0.0015 ft at the tip.

To show that realistic engineering systems can be analyzed using the present approach, we mount the composite box beam to a motor along with a weight 2 lbs at the tip to form a simple multibody dynamic system in Fig. 6. The motor will input a torque according to the schedule in Fig. 7 to the box beam at the root and the effect of gravity is taken into account with gravitational acceleration as  $32.2 \text{ ft/sec}^2$ . The displacements at the midspan and at the tip are plotted in Figs 8, 9, and 10, where solid line denotes the results at the tip and dashing line results at the midspan. It can be observed that the lateral displacements are much larger than axial displacements. The horizontal displacement assume a periodic shape opposite in sign to the applied torque. The vertical displacement is negative mainly due to the effect of gravity.

### Conclusion Remarks

This paper introduces a new concept for simulation of multibody systems with composite dimensionally reducible components using efficient high-fidelity structural models of VABS for composite beams and VAPAS for composite plates/shells. Powered with VABS and VAPAS, comprehensive multibody codes can be used to efficiently yet accurately design and analyze engineering systems involving composite components. The theoretical foundation and examples are provided to connecting VABS/VAPAS

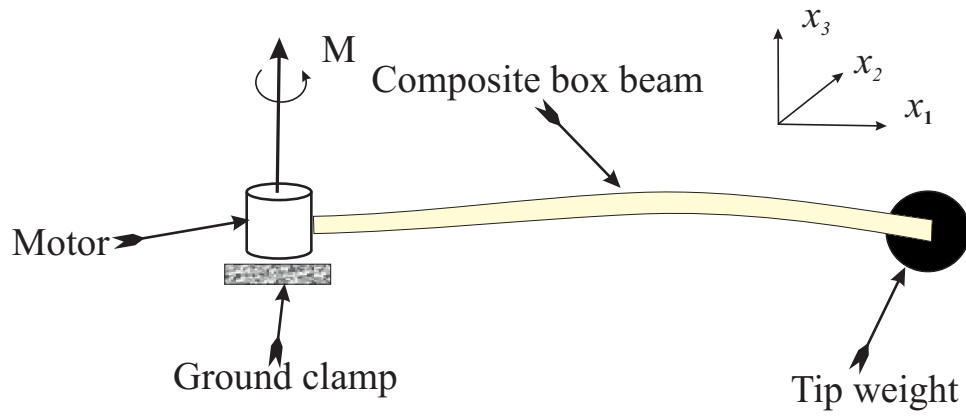


**Fig. 6** The composite box beam with a tip weight driven by a motor

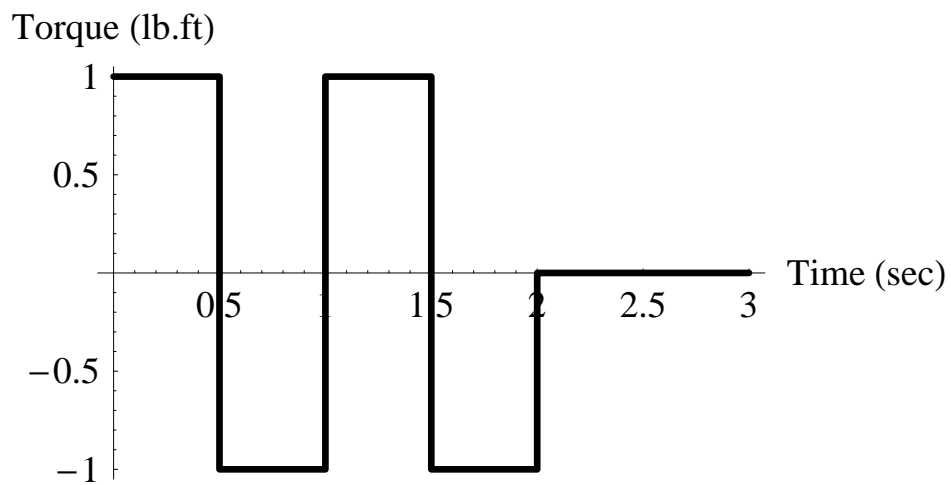


**Fig. 7** The periodic torque applied by the motor

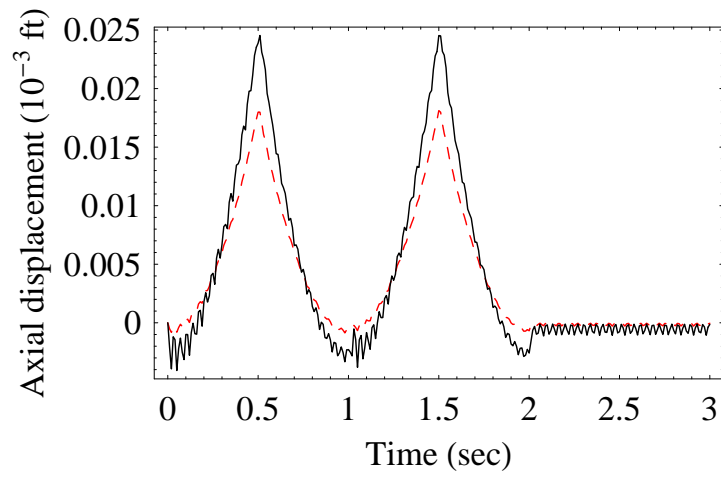


**Fig. 8** Time history of axial displacement. Solid line: at the tip; dashed line: at the mid-span

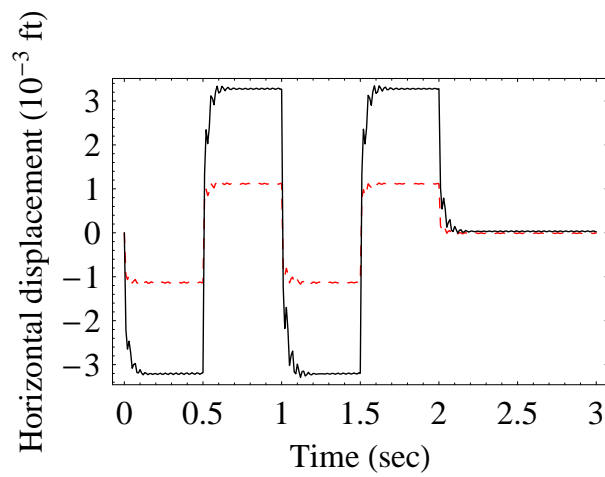


**Fig. 9** Time history of horizontal displacement. Solid line: at the tip; dashed line: at the mid-span

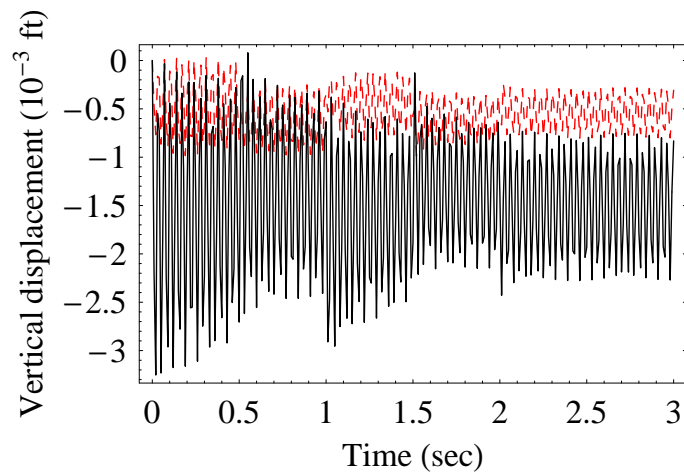


**Fig. 10** Time history of vertical displacement. Solid line: at the tip; dashed line: at the mid-span

with flexible multibody codes. It has been shown that various analysis such as static deformation, buckling/postbuckling, vibration, and others can be handled within the same unified approach. It has also be demonstrated that the same structure (such as composite beams having plate/shell type geometry) can be analyzed using several models including VABS beam models, VAPAS plate models, or 3D FEM. The choice depends on required accuracy and efficiency of particular problems. Connecting VABS and VAPAS with flexible multibody codes makes it possible to carry out authentic simulation for real engineering systems involving composite components. Numerous results presented in this work can be used as as assessment for other methods dealing with composite structures.

### Acknowledgements

This research is supported by the Space Dynamics Laboratory (SDL) at Utah State University (USU) under Skunk Works grant and Enabling Technologies grant. The views and conclusions contained herein are those of the author and should not be interpreted as necessarily representing the official policies or endorsement, either expressed or implied, of SDL or USU.

### References

- <sup>1</sup>Noor, A. K., and Burton, W. S., "Assessment of Computational Models for Multilayered Composite Shells," *Applied Mechanics Review*, Vol. 43, (4), 1990, pp. 67–96.
- <sup>2</sup>Noor, A. K., and Malik, M., "An Assessment of Five Modeling Approaches for Thermo-mechanical Stress Analysis of Laminated Composite Panels," *Computational Mechanics*, Vol. 25, (1), 2000, pp. 43–58.
- <sup>3</sup>Ghugal, Y., and Shimpi, R., "A Review of Refined Shear Deformation Theories for Isotropic and Anisotropic Laminated Beams," *Journal of Reinforced Plastics and Composites*, Vol. 20, (3), 2001, pp. 255–272.
- <sup>4</sup>Berdichevsky, V. L., "Variational-symptotic Method of Constructing a Theory of Shells," *PMM*, Vol. 43, (4), 1979, pp. 664–687.
- <sup>5</sup>Cesnik, C. E. S., and Hodges, D. H., "VABS: A New Concept for Composite Rotor Blade Cross-Sectional Modeling," *Journal of the American Helicopter Society*, Vol. 42, (1), 1997, pp. 27–38.
- <sup>6</sup>Yu, W., Hodges, D. H., Volovoi, V. V., and Cesnik, C. E. S., "On Timoshenko-like Modeling of Initially Curved and Twisted Composite Beams," *International Journal of Solids and Structures*, Vol. 39, (19), 2002, pp. 5101–5121.
- <sup>7</sup>Yu, W., Hodges, D. H., and Volovoi, V. V., "Asymptotic Construction of Reissner-like Models for Composite Plates with Accurate Strain Recovery," *International Journal of Solids and Structures*, Vol. 39, (20), 2002, pp. 5185–5203.
- <sup>8</sup>Yu, W., and Hodges, D. H., "An Asymptotic Approach for Thermoelastic Analysis of Laminated Composite Plates," *Journal of Engineering Mechanics*, Vol. 130, (5), 2004, pp. 531–540.
- <sup>9</sup>Yu, W., Hodges, D. H., and Volovoi, V. V., "Asymptotic Generalization of Reissner-Mindlin Theory: Accurate Three-dimensional Recovery for Composite Shells," *Computer Methods in Applied Mechanics and Engineering*, Vol. 191, (44), 2002, pp. 5087–5109.
- <sup>10</sup>Pagano, N. J., "Exact Solutions for Composite Laminates in Cylindrical Bending," *Journal of Composite Materials*, Vol. 3, 1969, pp. 398–411.
- <sup>11</sup>Le, K. C., *Vibrations of Shells and Rods*, Springer, Germany, 1999.

<sup>12</sup>Yu, W., and Hodges, D. H., “Generalized Timoshenko Theory of the Variational Asymptotic Beam Sectional Analysis,” *Journal of the American Helicopter Society*, Vol. 50, (1), 2005, pp. 46–55.

<sup>13</sup>Yu, W., Hodges, D. H., Volovoi, V. V., and Fuchs, E. D., “The Vlasov Theory of the Variational Asymptotic Beam Sectional Analysis,” *Thin-Walled Structures*, Vol. 43, (9), 2005, pp. 1493–1511.

<sup>14</sup>Abarcar, R., and Cunniff, P., “The Vibration of Cantilever Beams of Fiber Reinforced Material,” *Journal of Composite Materials*, Vol. 6, (10), 1972, pp. 504–517.

<sup>15</sup>Hodges, D. H., Atilgan, A. R., Fulton, M. V., and Rehfield, L. W., “Free-Vibration Analysis of Composite Beams,” *Journal of the American Helicopter Society*, Vol. 36, (3), 1991, pp. 36–47.

<sup>16</sup>Jung, S. N., Nagaraj, V. T., and Chopra, I., “Refined Structural Dynamics Model for Composite Rotor Blades,” *AIAA Journal*, Vol. 39, (2), 2001, pp. 339–348.

<sup>17</sup>Mitra, M., Gopalakrishnan, S., and Bhat, M., “A New Super Convergent Thin-walled Composite Beam Element for Analysis of Box Beam Structures,” *International Journal of Solids and Structures*, Vol. 41, (5-6), 2004, pp. 1491–1518.

<sup>18</sup>Chandra, R., and Chopra, I., “Experimental-Theoretical Investigation of the Vibration Characteristics of Rotating Composite Box Beams,” *Journal of Aircraft*, Vol. 29, (4), 1992, pp. 657–664.

<sup>19</sup>Smith, E. C., and Chopra, I., “Formulation and Evaluation of an Analytical Model for Composite Box-Beams,” *Journal of the American Helicopter Society*, Vol. 36, (3), 1991, pp. 23–35.

<sup>20</sup>Popescu, B., and Hodges, D. H., “On Asymptotically Correct Timoshenko-like Anisotropic Beam Theory,” *International Journal of Solids and Structures*, Vol. 37, (3), 2000, pp. 535–558.